

RESEARCH ARTICLE

OBE3 and WUS Interaction in Shoot Meristem Stem Cell Regulation

Ta-Fang Lin¹, Shunsuke Saiga², Mitsutomo Abe³, Thomas Laux^{1*}

1 BIOS Centre for Biological Signalling Studies, Faculty of Biology, University of Freiburg, Schaezlestrasse 1, 79104, Freiburg, Germany, **2** Laboratory of Biochemistry, Wageningen University, Dreijenlaan 3, 6703 HA, Wageningen, The Netherlands, **3** Department of Biological Sciences, Graduate School of Science, The University of Tokyo, 7-3-1 Hongo, Bunkyo-ku, Tokyo, 113-0033, Japan

* laux@biologie.uni-freiburg.de



OPEN ACCESS

Citation: Lin T-F, Saiga S, Abe M, Laux T (2016) OBE3 and WUS Interaction in Shoot Meristem Stem Cell Regulation. PLoS ONE 11(5): e0155657. doi:10.1371/journal.pone.0155657

Editor: Hector Candela, Universidad Miguel Hernández de Elche, SPAIN

Received: February 12, 2016

Accepted: May 2, 2016

Published: May 19, 2016

Copyright: © 2016 Lin et al. This is an open access article distributed under the terms of the [Creative Commons Attribution License](https://creativecommons.org/licenses/by/4.0/), which permits unrestricted use, distribution, and reproduction in any medium, provided the original author and source are credited.

Data Availability Statement: All relevant data are within the paper and its Supporting Information files.

Funding: This research was partially supported by grants from the Ministry of Education, Culture, Sports, Science and Technology of Japan (<http://www.mext.go.jp/english/>) to M.A. and mainly by grants from Deutsche Forschungsgemeinschaft [SFB592 (<http://www.sfb592.uni-freiburg.de/>)] and BMBF-FRISYS (<http://www.bioinf.uni-freiburg.de/Research/bmbf-frisys.html>) to T.L. The article processing charge was funded by the German Research Foundation (DFG) and the Albert Ludwigs University Freiburg in the funding programme Open Access Publishing. The funders had no role in study design, data collection

Abstract

The stem cells in the shoot apical meristem (SAM) are the origin of all above ground tissues in plants. In *Arabidopsis thaliana*, shoot meristem stem cells are maintained by the homeobox transcription factor gene *WUS* (*WUSCHEL*) that is expressed in cells of the organizing center underneath the stem cells. In order to identify factors that operate together with *WUS* in stem cell maintenance, we performed an EMS mutant screen for modifiers of the hypomorphic *wus-6* allele. We isolated the *oberon3-2* (*obe3-2*) mutant that enhances stem cell defects in *wus-6*, but does not affect the putative null allele *wus-1*. The *OBE3* gene encodes a PHD (Plant Homeo Domain) protein that is thought to function in chromatin regulation. Single mutants of *OBE3* or its closest homolog *OBE4* do not display any defects, whereas the *obe3-2 obe4-2* double mutant displays broad growth defects and developmental arrest of seedlings. Transcript levels of *WUS* and its target gene in the stem cells, *CLAVATA3*, are reduced in *obe3-2*. On the other hand, *OBE3* and *OBE4* transcripts are both indirectly upregulated by ectopic *WUS* expression. Our results suggest a positive feedback regulation between *WUS* and *OBE3* that contributes to shoot meristem homeostasis.

Introduction

Postembryonic growth and iterative organ formation of higher plants rely on the activity of pluripotent stem cells in organogenic centers, the meristems. The shoot meristem that will give rise to the above ground organs has been extensively studied in the model plant *Arabidopsis thaliana*. The homeodomain transcription factor *WUS* is expressed in the organizing center (OC) underneath the stem cells [1] where it directly represses cytokinin response inhibitors [2] and, after moving into the overlying stem cells [3, 4], represses cell differentiation and activates expression of the signal peptide *CLV3* [4–6]. *CLV3* in turn represses *WUS* transcription via *CLV1/CLV2*-CRN receptor-like kinases to delimit the size of the OC [6–8]. This negative feedback loop balances stem cell maintenance and differentiation [7]. The *WUS/CLV3* loop also functions to maintain stem cells of the floral meristems [6, 7]. In contrast to the indeterminate

and analysis, decision to publish, or preparation of the manuscript.

Competing Interests: The authors have declared that no competing interests exist.

shoot meristem, WUS in the determinate floral meristem also activates the gene encoding the MADS domain protein AGAMOUS (AG) that in turn terminates WUS expression and thus floral meristem growth [9–11]. In addition to its function in stem cell regulation, WUS is also required for the development of the female and male gametes [12–14]. However, CLV3 signaling does not appear to be targeted by WUS in these cases.

Although in the recent years, many studies identified further components affecting WUS/CLV3 homeostasis [3, 15–23], how WUS maintains stem cells remains enigmatic.

In order to find hitherto undiscovered factors involved in the WUS-mediated stem cell regulation, we used a sensitized mutant screen for genetic modifiers of the hypomorphic *wus-6* allele [21, 24]. Here we report the isolation of the *wus enhancer 9* (*wen9*) mutant that enhances stem cell defects in *wus-6*. We show by positional cloning that *wen9* is an allele of the *OBE3* gene, and characterize its function together with its closest homologue *OBE4* in the shoot meristem.

Results

wen9 enhances inflorescence shoot meristem defects of *wus-6*

The putative null allele *wus-1* causes premature termination of stem cells in the primary shoot meristem during embryogenesis, resulting in a flat apex of partially differentiated cells at the seedling stage [6]. Consequently, seedlings lack any true leaves at 10 days after germination (Fig 1B). Postembryonically initiated shoot meristems terminate after the formation of a few leaves, resulting in a stop-and-go phenotype (Fig 1C), and the seldom formed floral meristems give rise to 4 sepals, 4 petals, and a single stamen before premature termination (Fig 1D). The intermediate *wus-6* allele causes reduced WUS expression levels, and the primary seedling shoot meristem and floral meristem prematurely terminate indistinguishably to *wus-1* (Fig 1B and 1D; [21, 24]). In contrast to *wus-1*, however, postembryonically initiated *wus-6* shoot meristems grow indeterminately and give rise to many floral meristems (Fig 1C; Tables 1 and 2). The *wus-7* allele carries a missense mutation in the homeodomain and represents the weakest known *wus* allele [25]. *wus-7* seedlings form several rosette leaves before the primary shoot meristem terminates (Fig 1B) and axillary shoot meristems form indeterminate shoots carrying complete flowers (Fig 1C and 1D; Table 2).

In order to identify factors that cooperate with WUS in stem cell maintenance, we searched for EMS mutants that modify the stem cell defects of the intermediate allele *wus-6*. One of the isolated enhancers, *wus enhancer 9* (*wen9*), was mapped to a 97 kb region between position 5001124 and 5098789 on chromosome 1, and a nonsense mutation was identified in the predicted first exon of locus AT1G14740. The encoded protein OBERON3 (OBE3) [26], also named TITANIA1 (TTA1) [27], is 733 amino acids in size and contains a potential PHD (plant homeo domain) DNA binding domain (Fig 1A). The *wen9* mutation introduces a stop codon after the PHD domain at amino acid position 518. OBE3 transcript levels are reduced in *wen9* to about half of the wild-type level (S1 Fig). Transformation with a 4.6 kb genomic OBE3 fragment (Fig 1A) suppressed the enhanced phenotype of *wen9 wus-6* plants (S1 Table; S4 Fig) and two independent T-DNA insertion mutants in the OBE3 locus enhance *wus-6* similar to *wen9*, albeit to a weaker extent (S2 Table; S5 Fig). We thus conclude that the mutation in OBE3 caused the enhanced phenotype and assigned *wen9* as *obe3-2*.

To investigate the genetic interaction between WUS and OBE3, we analyzed double mutants between different *wus* alleles and the *obe3-2* mutant. Development of the homozygous *obe3-2* single mutant is indistinguishable from wild type (Figs 1B–1D and 2A). The *obe3-2* mutation does not affect the seedling phenotypes of *wus-1*, -6, or -7 (Fig 1B; Table 1). However, it strongly reduces the postembryonic formation of inflorescence stems in all combinations

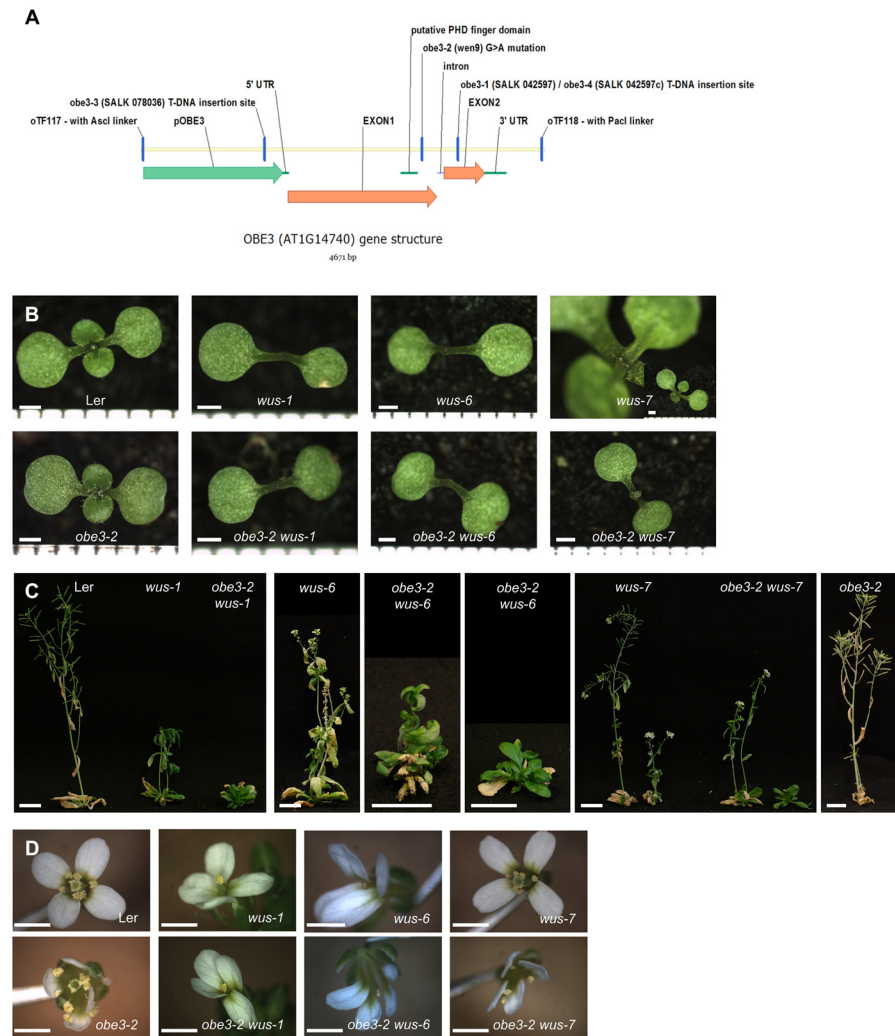


Fig 1. OBE3 gene structure and mutant phenotypes. (A) Structure of the OBE3 gene. The upstream region used for the complementation is shown in green. (B-D) Phenotypes of the denoted genotypes of 10-day-old seedlings (B), shoots (C), and flowers (D). Scale bars: 1 mm (B, D), 2 cm (C).

doi:10.1371/journal.pone.0155657.g001

(Fig 1C; Table 1) and causes the formation of leaves in a disorganized (= *wuschel*-like) pattern. In cases where flowers are made, *obe3-2* does not further enhance the already early termination of *wus-1* and *wus-6* floral meristems, but causes premature termination of *wus-7* floral meristems (Fig 1D; Table 2).

In summary, residual WUS activity in hypomorphic *wus* alleles requires OBE3 for maintenance of inflorescence meristems (*wus-6* and *wus-7*) and floral meristems (*wus-7*).

OBE3 functions redundantly with OBE4

Because the *obe3-2* single mutant does not display any developmental defect, we asked whether related genes might mask its function. To this end, we isolated an insertion mutant in the closest OBE3 homolog OBE4, also named TITANIA2 (TTA2) [27]. The *obe4-2* (SAIL_827_F11) mutation disrupts exon1, suggesting that it is a severe loss of function allele (S2 Fig). OBE4 transcript levels are reduced in *obe4-2* to about half of the wild-type level (S1 Fig). *obe4-2* single mutants are indistinguishable from the Col wild type (Fig 2A).

Table 1. *obe3-2* enhances the meristem defects of weak and intermediate *wus* alleles.

genotype of mother plant	n	ng	% of phenotype (of germinated seeds)								arrest ²
			seedling (10 DAG)				shoot (51DAG)				
			wt-like	<i>wus-7</i> like	<i>wus-1</i> like	retard ¹	wt-like	<i>wus-6</i> like	<i>wus-1</i> like	disorganized leaves, no stem	
<i>Ler</i>	244	42	99.5	0.0	0.0	0.5	99.0	0.0	0.0	0.0	1.0
<i>obe3-2</i>	51	2	98.0	0.0	0.0	2.0	98.0	0.0	0.0	0.0	2.0
<i>wus-1/+</i>	202	3	69.9	0.0	28.1	2.0	68.8	1.5	24.6	4.0	1.1
<i>obe3-2 wus-1/+</i>	205	2	75.9	0.0	20.7	3.4	69.5	3.9	1.5	19.7	5.4
<i>wus-6/+</i>	245	0	73.5	0.0	25.3	1.2	73.1	25.7	0.0	0.0	1.2
<i>obe3-2 wus-6/+</i>	212	1	74.4	0.0	24.2	1.4	74.4	0.0	0.0	23.7	1.9
<i>wus-7/+</i>	237	2	94.0	5.6	0.0	0.4	79.6	19.5	0.0	0.0	0.9
<i>obe3-2 wus-7/+</i>	228	4	93.8	4.9	0.4	0.9	75.4	19.2	0.0	4.5	0.9

Seedling phenotype classes: wt-like, shoot meristem forming a rosette of leaves; *wus-7*-like; shoot meristem termination after true leaves have been formed, *wus-1*-like: shoot meristem termination without any leaves.

Shoot phenotype classes: wt-like, rosette, indeterminate inflorescence; *wus-6*-like, disorganized leaves, indeterminate inflorescence; *wus-1*-like, disorganized leaves, stop-and-go inflorescence rarely forming flowers.

DAG, days after germination; n, number of plants analyzed; ng, not germinated;

¹, retard: small whitish seedlings with retarded growth and cotyledons only.

², arrest: plants stopped development at seedling stage.

Chi-square test results for the seedling phenotype difference between:

wus-1/+ vs *obe3-2 wus-1/+*, p>0.05, not significant

wus-6/+ vs *obe3-2 wus-6/+*, p>0.05, not significant

wus-7/+ vs *obe3-2 wus-7/+*, p>0.05, not significant

Chi-square test results for the shoot phenotype difference between:

wus-1/+ vs *obe3-2 wus-1/+*, p<0.0001, highly significant

wus-6/+ vs *obe3-2 wus-6/+*, p<0.0001, highly significant

wus-7/+ vs *obe3-2 wus-7/+*, 0.01<p<0.05, significant

doi:10.1371/journal.pone.0155657.t001

In the segregating progeny of an *obe3-2/+ obe4-2/+* mother plant, we found 2.8% (n = 143) very small seedlings with partially fused cotyledons and without any true leaves, did not develop further, and were genotyped as homozygous double mutants by PCR (Fig 2B). By contrast, all *obe3-2 obe4-2/+* plants identified by PCR (9.8%, n = 143) formed true leaves, but

Table 2. Flower phenotypes of *obe3-2 wus-1*, *obe3-2 wus-7* and *obe3-2 wus-6*.

Genotype	n flowers	stamens	carpels
wild type (<i>Ler</i>)	20	6.0±0.0	2.0±0.0
<i>obe3-2</i>	20	6.0±0.0	1.8±0.6
<i>wus-1</i>	8	1.0±0.0	0.0±0.0
<i>obe3-2 wus-1</i>	3	1.0±0.0	0–0±0.0
<i>wus-6</i>	20	1.0±0.0	0.0±0.0
<i>obe3-2 wus-6</i>	3	1.0±0.0	0.0±0.0
<i>wus-7</i>	15	5.9±0.6	1.6±0.8
<i>obe3-2 wus-7</i>	20	4.0±0.0	0.2±0.6

At 79 DAG (except the *obe3-2 wus-6* at 100DAG), opened flowers were taken from the genotyped plants and the organ numbers were counted. Organ numbers in first and second whorls were 4 sepals and 4 petals, respectively, for all genotypes.

doi:10.1371/journal.pone.0155657.t002

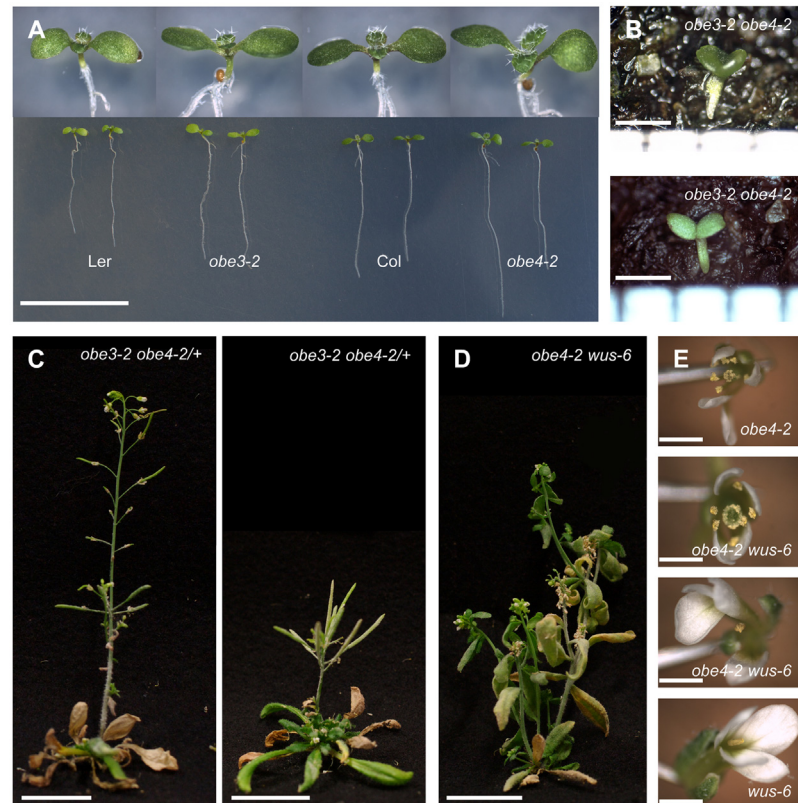


Fig 2. Genetic combinations of *obe3-2* and *obe4-2*. (A) Plants of *obe3-2* and *obe4-2* single mutants are indistinguishable from wild type. (B) *obe3-2 obe4-2* seedlings that did not develop further. (C) *obe3-2 obe4-2/+* plants displayed two phenotypic classes at 60 DAG. (D) *obe4-2 wus-6* plant displayed *wus-6*-like shoot formation at 60 DAG. (E) *obe4-2 wus-6* plant produced complete flowers and *wus-1* like flowers. Scale bars: 2 cm (A, C and D), 1 mm (B and E).

doi:10.1371/journal.pone.0155657.g002

display severe growth retardation (Fig 2C), whereas the remaining segregating sibling plants look like wild type. We independently confirmed these results with the *obe3-1 obe4-1* combination (S3 Fig). Thus, *OBE3* and *OBE4* are redundantly required for plant growth.

obe4-2 wus-6 double mutants are indistinguishable from *wus-6*, with the exceptions that *obe4-2 wus-6* inflorescences produced less than 10 siliques (data not shown) and that all double mutant plants (n = 6) were mosaics carrying both, wild-type-like complete flowers (40/170) and *wus-1*-like incomplete flowers (130/170; Fig 2D and 2E). Thus, in contrast to *obe3-2*, the *obe4-2* mutation restores carpel and seed development in *wus-6*, suggesting that in floral meristems, *WUS* and *OBE4* act oppositely.

Mutual expression regulation between *WUS* and *OBE3*

In order to investigate whether the expression levels of *WUS* and *CLV3* genes are altered, we performed qRT-PCR with the 7 day-old *obe3-2* and *obe4-2* seedlings. *WUS* and *CLV3* mRNA levels are significantly reduced in *obe3-2* (0.43 and 0.45 fold, respectively) compared to the *Ler* wild type, whereas *ARR7* mRNA levels appear increased (Fig 3A). In a converse experiment, *WUS* mRNA level is increased after induction of *p35S:cOBE3-GR* expression and this effect is suppressed in the presence of cycloheximide, whereas mRNA levels of *CLV3*, *STM*, and *ARR7* are not significantly changed (Fig 3B). In contrast to *obe3-2*, expression levels of *WUS* or *CLV3*

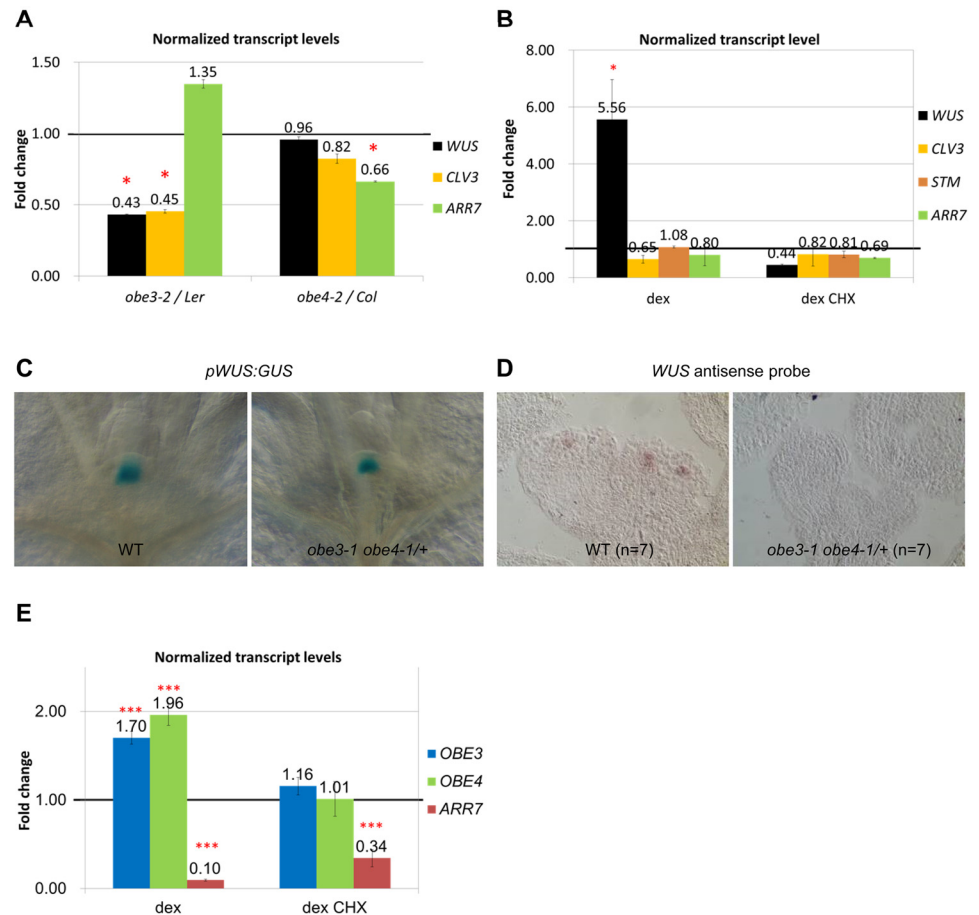


Fig 3. Changes of transcripts in *obe3-2* and *obe4-2*. (A) Transcript levels of 7-day-old seedlings as indicated. Error bars represent SE. (B) After induction of *OBE3* overexpression, mRNA levels of *WUS* are increased, whereas mRNA levels of *CLV3*, *STM*, and *ARR7* are unchanged in 7-day-old seedling. Error bars represent SD. (C) *pWUS:GUS* expression in 6-day-old *obe3-1 obe4-1/+* seedlings is confined to the OC as in the wild type. (D) *WUS* mRNA is undetectable by *in situ* hybridization in *obe3-1 obe4-1/+* floral meristems of 30-day-old plants. (E) *WUS* overexpression upregulates *OBE3* and *OBE4* mRNA levels in 7-day-old seedlings. *ARR7* expression is used as a control. Error bars represent SD. Relative mRNA levels compared to the mock control are shown. *, $p < 0.05$, calculated from C_p' values; ***, $p < 0.001$, calculated from C_p' values.

doi:10.1371/journal.pone.0155657.g003

genes are not significantly changed in *obe4-2* (Fig 3A), but the *ARR7* mRNA level is reduced (Fig 3A). In summary, *OBE3* is required for normal *WUS* and *CLV3* expression.

Because double mutant plants are severely retarded, we analyzed the *WUS* expression pattern in *obe3-1 obe4-1/+* plants. In 6-day-old seedlings, expression of the *pWUS:GUS* (Fig 3C) reporter is confined to the OC of *obe3-1 obe4-1/+* plants as in the wild type. However, in 20-day-old inflorescences, *WUS* expression is not detectable in *obe3-1 obe4-1/+* (genotyped by PCR) inflorescence and floral meristems unlike in the wild type (Fig 3D).

In order to address whether *WUS* affects *OBE3/OBE4* transcript levels, we analyzed the effects of inducible *WUS* activity. After induction of *p35S:WUS-GR* plants with dexamethasone, mRNA levels of *OBE3* and *OBE4* are upregulated, and this effect is suppressed in the presence of cycloheximide (Fig 3E). The direct *WUS* target in the shoot meristem, *ARR7* [2], is used as a control for *WUS-GR* induction. Upregulation of *OBE3* and *OBE4* expression by *WUS* is also suggested by published microarray data (S3 Table). Thus, *WUS* activity is sufficient to

induce *OBE3/OBE4* expression by an indirect mechanism. However, we did not detect any abnormal phenotype in *p35S:cOBE3* or *p35S:cOBE3-GR* plants.

Overexpression of *OBE3* alleviates shoot meristem but not floral meristem defects of *wus-1*

Because *WUS* overexpression can upregulate *OBE3*, we asked whether forced expression of *OBE3* can overcome the absence of *WUS* activity and expressed *p35S:cOBE3* in *wus-1*. When comparing segregating *p35S:cOBE3 wus-1/+* plants with *wus-1* empty vector controls, we find that the number of seedlings lacking the shoot meristem are reduced (10.3% vs. 28.5%) whereas seedlings with weak shoot meristem defects are increased (20.8% vs. 6.0%; Fig 4A, S4 Table). Furthermore, postembryonic shoot formation is increased (29.2% vs. 14.7%; S4 Table). The difference between *p35S:cOBE3 wus-1/+* and empty vector *wus-1/+* control is highly significant in both seedling and shoot stages (both Chi square, $p < 0.0001$). By contrast, defective *wus-1*

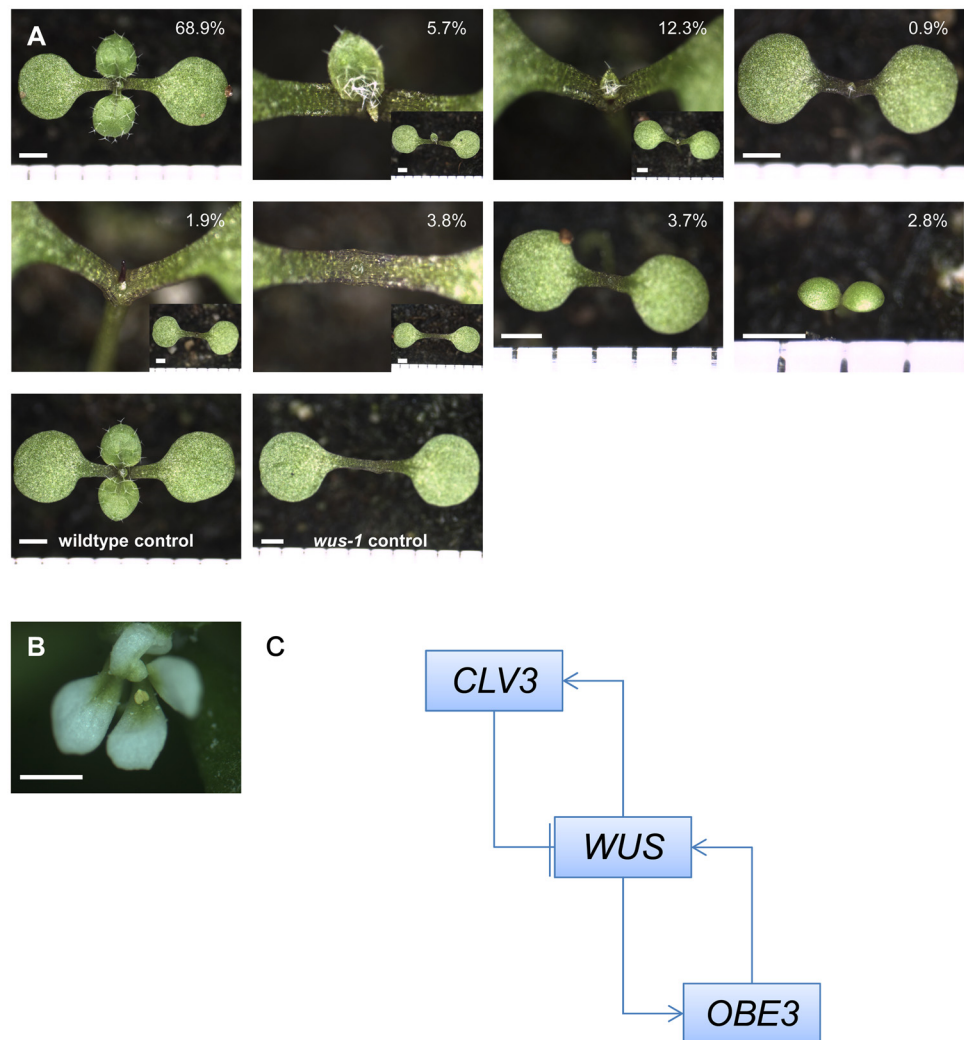


Fig 4. *p35S:cOBE3* expression partially suppresses *wus-1* defects. (A) Phenotypes of segregating seedlings in the progeny of a *p35S:cOBE3 wus-1/+* mother plant. (B) *p35S:cOBE3 wus-1* plants produce *wus-1*-like flowers. (C) Model for *WUS-OBE3* interaction. Scale bars: 1 mm.

doi:10.1371/journal.pone.0155657.g004

flower development is not altered by *p35S:cOBE3* (Fig 4B). Thus, *OBE3* activity can partially replace *WUS* activity in seedling and inflorescence shoot meristems, but not in the floral meristem.

Discussion

Stem cell homeostasis requires the balanced activities of a complex network of regulatory factors. Despite strong advances, our knowledge of regulatory pathways is still fragmentary with many components unknown. This is due in part to the fact that a limited number of mutants display informative stem cell phenotypes. Furthermore, many other essential stem cell factors may remain undiscovered due to genetic redundancy or pleiotropic mutant phenotypes. Here we used a modifier screen to overcome this problem and discovered the *obe3-2* mutant as an enhancer of the hypomorphic *wus-6* allele.

What is the developmental nature of the *WUS-OB3* interaction?

The role of *WUS* in stem cell maintenance can be observed at several developmental stages. Mature *wus-1* embryos and seedlings lack shoot meristem stem cells and display differentiated cells instead. Postembryonically formed adventitious meristems terminate prematurely after forming a few leaves. Only occasionally an inflorescence is formed, but it terminates prematurely after formation of 1–3 flowers, which in turn terminate prematurely after a single first anther. Whereas seedling and floral meristems appear to absolutely require *WUS* activity, the occasional formation of inflorescences suggests that at this stage other factors can sustain stem cells for some time [21]. Although *OBE3* is ubiquitously expressed [27], the *obe3-2* mutation enhances only the premature vegetative shoot meristem termination in *wus-1* and thus represents one of these additional factors. In the hypomorphic allele *wus-6*, *obe3-2* causes premature termination of the inflorescence meristem indistinguishable to *wus-1*. Finally, in combination with *wus-7*, which as a single mutant displays higher floral meristem activity compared to *wus-1* and *wus-6*, *obe3-2* enhances premature termination of the floral meristem. These results indicate that in addition to the seedling phase, *OBE3* is required for residual *WUS* activity of hypomorphic *wus* alleles in inflorescence and floral meristems. By contrast, *obe3-2* does not enhance *wus* defects in embryonic shoot meristem formation.

Curiously, despite their redundancy in the shoot meristem, *obe3* enhances *wus* flower termination whereas *obe4* mutant suppresses it. One possible reason for this particular behavior might be that in *obe3-1* and *obe3-2* mutants, the C-terminal region of *OBE3* is disrupted and the PHD domain is still intact, whereas in *obe4-1* and *obe4-2* mutants the PHD domain is disrupted. Alternatively, both wild-type proteins might have divergent functions specifically in floral meristems.

Considering the ubiquitous expression of *OBE3*, it is noteworthy that the *obe3-2* mutation reduces the organ number only of the two inner whorls of *wus-7* but does not affect the perianth. A plausible explanation is that *WUS*-mediated stem cell maintenance is only required to provide the cells for the inner two whorls, whereas perianth organs appear to consume the cells present in the initial floral meristem formed independently of *WUS*, as described previously [6].

What is the genetic nature of the *WUS-OB3* interaction?

Based on our mutant analysis and expression studies, *OBE3* appears to act downstream of *WUS*. On the other hand, *WUS* expression levels are reduced in *obe3-2* mutants and increased by *OBE3* overexpression from the ubiquitous 35S promoter. The reduction of *pWUS:GUS* expression in the shoot meristem of *obe3-1 obe4-1/+* mutants and the requirement of *OBE3* in

wus hypomorphs suggest that this is also the case in shoot meristem regulation. One plausible interpretation of this data is that *WUS* and *OBE3* reinforce each other's expression in a positive feedback loop (Fig 4C), albeit this effect seems moderate.

OBE3 is a member of a small group of related proteins and, together with its closest homolog *OBE4*, is redundantly required for plant growth, consistent with previous observations [27]. The seedling lethality of *obe3-2 obe4-2* double mutants suggests that both genes are involved in several processes other than shoot meristem regulation. Likewise, *obe1 obe2* [28] displays seedling lethality, but not any other *obe* double mutant combinations, indicating two pairs of redundant functions in this group, *OBE1,2* and *OBE3,4*. In contrast to *obe3-2 wus-6* plants, *obe4-2 wus-6* double mutants have *wus-6*-like inflorescences and partially restored floral organs and seed production. This indicates that *OBE3* and *OBE4*, in addition to their redundant functions in general growth control, have opposite roles at least in floral meristems.

What is a possible molecular basis of interaction?

The upregulation of *OBE3* mRNA levels by *WUS* and vice versa is abolished by the presence of the protein inhibitor cycloheximide, suggesting that intermediate components are necessary. OBEs are PHD domain containing proteins, which originally were found by their homology to the Potyvirus VPg-interacting protein [29]. The PHD domain is reported to bind to potentially activating H3K4me2/3 modifications [30–34]. Further experiments are necessary to address how OBE affects *WUS* expression and vice versa and whether the enhancement of hypomorphic *wus* mutant defects by *obe3-2* can be attributed to the reduction of *WUS* expression levels.

Material and Methods

Plant materials and growth conditions

The *obe3-2* mutant was isolated from EMS-mutagenized populations in a *wus-6* background in *Ler* [25]. The insertion alleles *obe3-3*^{SALK_078036}, *obe3-4*^{SALK_042597c} and *obe4-2*^{SAIL_827_F11} in the *Col* background were identified from the SALIK collection [35] of T-DNA tagged lines and the SAIL collection [36], respectively. All other mutant alleles and transgenic lines used in this study are listed in S5 Table. For segregation analysis, entire siliques from genotyped mother plants were harvested and the seeds were sown in randomized schemes [37]. Plant growth conditions were as previously described [6].

Mapping, genetic analysis and PCR genotyping

The *wen9 wus-6/+* x *Col* cross was performed for map-based cloning. Among 12113 F2 plants from F1 parents genotyped as *wus-6/+*, we identified 446 plants (3.7%) with an enhanced phenotype. The *wen9* mutation was mapped with SSLP and dCAPS markers to a 97 kb region in chromosome 1 (between SNP CER465614 and CER424346). Sequencing of all 23 candidate loci in this region detected a mutation only in the *OBE3* gene. The identified G1554>A “stop” mutation is in exon1 of the predicted reading frame of locus AT1G14740. The primers *wen9-F* (5′ – CAGAGATGTTTGGATTTCGTTAAGGATGTTTTTGTGTGTTGCGCTAAGAATCG – 3′) and *wen9-R* (5′ – GAAATGTGATAAGAGAAGG – 3′) were used for genotyping PCRs (Ta 55°C). After TaqI restriction cleavage, the wild type displays a 300bp band, and *wen9* displays a 250bp and a 50bp band. Genotyping primers of other mutants including T-DNA lines used in this study are listed in S6 Table.

Preparation of constructs and selection of transformants

The genomic fragment including the intergenic region of *OBE3* was amplified by PCR from Ler and cloned as *pOBE3:gOBE3* in a *pGPTV-HPT*-based vector. The RALF11-03K20 cDNA clone from RIKEN BRC was used to amplify the full length cDNA by PCR for construct preparation. The cDNA fragments starting from ATG to the end of gene, with or without the stop codon, were cloned as: *p35S:cOBE3*, and *p35S:cOBE3-GR* respectively, in a *pGreenII*-based vector. *Arabidopsis* plants were transformed by floral dip, and T1 seeds were selected on plates with the respective antibiotics.

Quantitative RT-PCR analysis

Arabidopsis seeds were surface-sterilized with 1% hypochlorite for 10 minutes and washed two times with 70% ethanol. Sterilized seeds were sown on 1/2 MS plates, stratified for 3 days in the dark at 4°C and then grown in a Percival growth cabinet with constant illumination for 7 or 10 days. For all qRT-PCR experiments, 3 biological replicates with two technical replicates each were done.

For experiments without further treatment, seedlings were collected from the plates and frozen in liquid nitrogen immediately. For the induction experiments, dexamethasone (5 μM), with or without cycloheximide (50 μM) were applied by spraying the plates, and flooding the seedlings for 15 minutes. After removal of the liquid, seedlings were returned to the Percival growth cabinet for 4 hours before sample collection.

Total RNA was extracted from whole seedlings using the RNeasy[®] Mini kit (QIAGEN), followed by RQ1 RNase-Free DNase (Promega) treatment and reverse-transcribed with SuperScript III First-Strand Synthesis SuperMix for qRT-PCR (Invitrogen). Quantitative PCR was performed with the LightCycler[®] 480 system (Roche) coupled with SYBR Green I Master (Roche). For each qPCR reaction, 25 ng of cDNA was used. Transcript level analysis was carried out according to a published protocol [38]. For statistical analysis, ANOVA or *t*-tests were performed on Cp' values. The Cp' values were calculated after normalizing the Cp values with three independent reference genes, which passed the geNorm v3.5 [39] test. For graphic presentation, Normalized Relative Quantity (NRQ) was first rescaled by setting NRQ of mock treated wild-type samples as 1, then adjusted for the unspecific DEX effect and the transgene effect sequentially in order to calculate the transcript fold change. Fold changes were plotted as bar graphs. Primers used for quantitative PCR are listed in [S7 Table](#).

Supporting Information

S1 Fig. Transcript level of *OBE3* and *OBE4* is reduced in the corresponding mutants.
(TIF)

S2 Fig. Structure of *OBE4*.
(TIF)

S3 Fig. Genetic combinations of *obe3-1* and *obe4-1*.
(TIF)

S4 Fig. A genomic *OBE3* fragment suppresses the enhanced phenotype of *obe3-2 wus-6*.
(TIF)

S5 Fig. *OBE3* T-DNA insertion mutants enhance *wus-6* defects.
(TIF)

S1 Table. A genomic *gOBE3* fragment suppresses the effects of the *wen9* mutation.
(PDF)

S2 Table. *OBE3* T-DNA insertion lines enhance *wus-6*.
(PDF)

S3 Table. Microarray expression levels of *OBE* genes.
(PDF)

S4 Table. Phenotypes of segregating *p35S:cOBE3 wus-1/+* plants.
(PDF)

S5 Table. Mutants and Transgenic lines used in this study.
(PDF)

S6 Table. Primers used for genotyping mutant alleles.
(PDF)

S7 Table. Primers used for qPCR.
(PDF)

Acknowledgments

We thank SALK, ABRC, NASC and RIKEN BRC for providing seeds and cDNA clones. We thank members of the Laux laboratory for discussions. We thank Dr. Edwin Groot for proof-reading the manuscript and help in statistical analysis. This research was supported by grants from the Ministry of Education, Culture, Sports, Science and Technology of Japan to M.A. and from the Deutsche Forschungsgemeinschaft (SFB592 and BMBF-FRISYS) to T.L. The article processing charge was funded by the German Research Foundation (DFG) and the Albert Ludwigs University Freiburg in the funding programme Open Access Publishing.

Author Contributions

Conceived and designed the experiments: SS MA T-FL TL. Performed the experiments: SS T-FL. Analyzed the data: SS T-FL TL. Contributed reagents/materials/analysis tools: SS MA T-FL TL. Wrote the paper: T-FL TL. [Fig 3C and 3D](#), [S3 Fig](#): SS MA. Rest of the data: T-FL TL.

References

1. Mayer KFX, Schoof H, Haecker A, Lenhard M, Jürgens G, Laux T. Role of WUSCHEL in Regulating Stem Cell Fate in the *Arabidopsis* Shoot Meristem. *Cell*. 1998; 95(6):805–15. PMID: [9865698](#)
2. Leibfried A, To JP, Busch W, Stehling S, Kehle A, Demar M, et al. WUSCHEL controls meristem function by direct regulation of cytokinin-inducible response regulators. *Nature*. 2005; 438(7071):1172–5. PMID: [16372013](#).
3. Daum G, Medzihradzky A, Suzaki T, Lohmann JU. A mechanistic framework for noncell autonomous stem cell induction in *Arabidopsis*. *Proc Natl Acad Sci U S A*. 2014; 111(40):14619–24. Epub 2014/09/24. doi: [10.1073/pnas.1406446111](#) PMID: [25246576](#); PubMed Central PMCID: PMC4210042.
4. Yadav RK, Perales M, Gruel J, Girke T, Jonsson H, Reddy GV. WUSCHEL protein movement mediates stem cell homeostasis in the *Arabidopsis* shoot apex. *Genes Dev*. 2011; 25(19):2025–30. Epub 2011/10/08. doi: [10.1101/gad.17258511](#) PMID: [21979915](#); PubMed Central PMCID: PMC3197201.
5. Yadav RK, Girke T, Pasala S, Xie M, Reddy GV. Gene expression map of the *Arabidopsis* shoot apical meristem stem cell niche. *Proc Natl Acad Sci U S A*. 2009; 106(12):4941–6. PMID: [19258454](#). doi: [10.1073/pnas.0900843106](#)
6. Laux T, Mayer KF, Berger J, Jurgens G. The WUSCHEL gene is required for shoot and floral meristem integrity in *Arabidopsis*. *Development*. 1996; 122(1):87–96. PMID: [8565856](#).

7. Schoof H, Lenhard M, Haecker A, Mayer KF, Jurgens G, Laux T. The stem cell population of Arabidopsis shoot meristems is maintained by a regulatory loop between the CLAVATA and WUSCHEL genes. *Cell*. 2000; 100(6):635–44. PMID: [10761929](#).
8. Brand U, Fletcher JC, Hobe M, Meyerowitz EM, Simon R. Dependence of stem cell fate in Arabidopsis on a feedback loop regulated by CLV3 activity. *Science*. 2000; 289:617–9. PMID: [10915624](#)
9. Lohmann JU, Hong RL, Hobe M, Busch MA, Parcy F, Simon R, et al. A molecular link between stem cell regulation and floral patterning in Arabidopsis. *Cell*. 2001; 105(6):793–803. Epub 2001/07/07. S0092-8674(01)00384-1 [pii]. PMID: [11440721](#).
10. Liu X, Kim YJ, Muller R, Yumul RE, Liu C, Pan Y, et al. AGAMOUS terminates floral stem cell maintenance in Arabidopsis by directly repressing WUSCHEL through recruitment of Polycomb Group proteins. *Plant Cell*. 2011; 23(10):3654–70. Epub 2011/10/27. tpc.111.091538 [pii]doi: [10.1105/tpc.111.091538](#) PMID: [22028461](#); PubMed Central PMCID: PMC3229141.
11. Lenhard M, Bohnert A, Jürgens G, Laux T. Termination of Stem Cell Maintenance in Arabidopsis Floral Meristems by Interactions between WUSCHEL and AGAMOUS. *Cell*. 2001; 105(6):805–14. PMID: [11440722](#)
12. Deyhle F, Sarkar AK, Tucker EJ, Laux T. WUSCHEL regulates cell differentiation during anther development. *Dev Biol*. 2007; 302(1):154–9. PMID: [17027956](#).
13. Groß-Hardt R, Lenhard M, Laux T. WUSCHEL signaling functions in interregional communication during Arabidopsis ovule development. *Genes & Development*. 2002; 16(9):1129–38. doi: [10.1101/gad.225202](#)
14. Lieber D, Lora J, Schrempf S, Lenhard M, Laux T. Arabidopsis WIH1 and WIH2 genes act in the transition from somatic to reproductive cell fate. *Curr Biol*. 2011; 21(12):1009–17. Epub 2011/06/11. S0960-9822(11)00542-2 [pii]doi: [10.1016/j.cub.2011.05.015](#) PMID: [21658947](#).
15. Zhao Z, Andersen SU, Ljung K, Dolezal K, Miotk A, Schultheiss SJ, et al. Hormonal control of the shoot stem-cell niche. *Nature*. 2010; 465(7301):1089–92. PMID: [20577215](#). doi: [10.1038/nature09126](#)
16. Kwon CS, Chen C, Wagner D. WUSCHEL is a primary target for transcriptional regulation by SPLAYED in dynamic control of stem cell fate in Arabidopsis. *Genes Dev*. 2005; 19(8):992–1003. PMID: [15833920](#).
17. Kieffer M, Stern Y, Cook H, Clerici E, Maulbetsch C, Laux T, et al. Analysis of the Transcription Factor WUSCHEL and Its Functional Homologue in Antirrhinum Reveals a Potential Mechanism for Their Roles in Meristem Maintenance. *Plant Cell*. 2006; 18(3):560–73. doi: [10.1105/tpc.105.039107](#) PMID: [16461579](#)
18. Tucker MR, Hinze A, Tucker EJ, Takada S, Jurgens G, Laux T. Vascular signalling mediated by ZWILLE potentiates WUSCHEL function during shoot meristem stem cell development in the Arabidopsis embryo. *Development*. 2008; 135(17):2839–43. PMID: [18653559](#). doi: [10.1242/dev.023648](#)
19. Gordon SP, Chickarmane VS, Ohno C, Meyerowitz EM. Multiple feedback loops through cytokinin signaling control stem cell number within the Arabidopsis shoot meristem. *Proc Natl Acad Sci U S A*. 2009; 106(38):16529–34. PMID: [19717465](#). doi: [10.1073/pnas.0908122106](#)
20. Yadav RK, Tavakkoli M, Reddy GV. WUSCHEL mediates stem cell homeostasis by regulating stem cell number and patterns of cell division and differentiation of stem cell progenitors. *Development*. 2010; 137(21):3581–9. Epub 2010/09/30. dev.054973 [pii]doi: [10.1242/dev.054973](#) PMID: [20876644](#).
21. Graf P, Dolzblasz A, Wurschum T, Lenhard M, Pfreundt U, Laux T. MGOUN1 encodes an Arabidopsis type IB DNA topoisomerase required in stem cell regulation and to maintain developmentally regulated gene silencing. *Plant Cell*. 2010; 22(3):716–28. PMID: [20228247](#). doi: [10.1105/tpc.109.068296](#)
22. Nimchuk ZL, Tarr PT, Ohno C, Qu X, Meyerowitz EM. Plant stem cell signaling involves ligand-dependent trafficking of the CLAVATA1 receptor kinase. *Curr Biol*. 2011; 21(5):345–52. PMID: [21333538](#). doi: [10.1016/j.cub.2011.01.039](#)
23. Chickarmane VS, Gordon SP, Tarr PT, Heisler MG, Meyerowitz EM. Cytokinin signaling as a positional cue for patterning the apical-basal axis of the growing Arabidopsis shoot meristem. *Proc Natl Acad Sci U S A*. 2012; 109(10):4002–7. Epub 2012/02/22. 1200636109 [pii]doi: [10.1073/pnas.1200636109](#) PMID: [22345559](#).
24. Hamada S, Onouchi H, Tanaka H, Kudo M, Liu Y-G, Shibata D, et al. Mutations in the WUSCHEL gene of *Arabidopsis thaliana* result in the development of shoots without juvenile leaves. *the Plant Journal*. 2000; 24(1):91–101. PMID: [11029707](#)
25. Graf P. Genetic modifiers of WUSCHEL function in Arabidopsis stem cell maintenance [Inaugural-Dissertation zur Erlangung der Doktorwürde]. Freiburg im Breisgau: Albert-Ludwigs-Universität; 2007.
26. Thomas CL, Schmidt D, Bayer EM, Dreos R, Maule AJ. Arabidopsis plant homeodomain finger proteins operate downstream of auxin accumulation in specifying the vasculature and primary root meristem. *the Plant Journal*. 2009; 59:426–36. doi: [10.1111/j.1365-3113X.2009.03874.x](#) PMID: [19392692](#)

27. Saiga S, Möller B, Watanabe-Taneda A, Abe M, Weijers D, Komeda Y. Control of embryonic meristem initiation in Arabidopsis by PHD-finger protein complexes. *Development*. 2012; 139(8):1391–8. doi: [10.1242/dev.074492](https://doi.org/10.1242/dev.074492) PMID: [22378640](https://pubmed.ncbi.nlm.nih.gov/22378640/)
28. Saiga S, Furumizu C, Yokoyama R, Kurata T, Sato S, Kato T, et al. The Arabidopsis OBERON1 and OBERON2 genes encode plant homeodomain finger proteins and are required for apical meristem maintenance. *Development*. 2008; 135:1751–9. doi: [10.1242/dev.014993](https://doi.org/10.1242/dev.014993) PMID: [18403411](https://pubmed.ncbi.nlm.nih.gov/18403411/)
29. Dunoyer P, Thomas C, Harrison S, Revers F, Maule A. A Cysteine-Rich Plant Protein Potentiates Potyvirus Movement through an Interaction with the Virus Genome-Linked Protein VPg. *Journal of Virology*. 2004; 78(5):2301–9. PMID: [14963126](https://pubmed.ncbi.nlm.nih.gov/14963126/)
30. Li H, Ilin S, Wang W, Duncan EM, Wysocka J, Allis CD, et al. Molecular basis for site-specific read-out of histone H3K4me3 by the BPTF PHD finger of NURF. *Nature, Letters*. 2006; 442:91–5.
31. Mellor J. It Takes a PHD to Read the Histone Code. *Cell*. 2006; 126:22–4. PMID: [16839870](https://pubmed.ncbi.nlm.nih.gov/16839870/)
32. Peña PV, Davrazou F, Shi X, Walter KL, Verkhusha VV, Gozani O, et al. Molecular mechanism of histone H3K4me3 recognition by plant homeodomain of ING2. *Nature, Letters*. 2006; 442:100–3.
33. Shi X, Hong T, Walter KL, Ewalt M, Michishita E, Hung T, et al. ING2 PHD domain links histone H3 lysine 4 methylation to active gene repression. *Nature, Letters*. 2006; 442:96–9.
34. Wysocka J, Swigut T, Xiao H, Milne TA, Kwon SY, Landry J, et al. A PHD finger of NURF couples histone H3 lysine 4 trimethylation with chromatin remodelling. *Nature, Letters*. 2006; 442:86–90.
35. Alonso JM, Stepanova AN, Leisse TJ, Kim CJ, Chen H, Shinn P, et al. Genome-wide insertional mutagenesis of Arabidopsis thaliana. *Science*. 2003; 301(5633):653–7. PMID: [12893945](https://pubmed.ncbi.nlm.nih.gov/12893945/).
36. Sessions A, Burkea E, Prestinga G, Auxb G, McElverb J, Pattonb D, et al. A High-Throughput Arabidopsis Reverse Genetics System. *The Plant Cell*. 2002; 14:2985–94. PMID: [12468722](https://pubmed.ncbi.nlm.nih.gov/12468722/)
37. Urbaniak GC, Plous S. Research Randomizer (Version 3.0)[Computer software]. Available: <http://www.randomizer.org/>. 2009. Epub 3.
38. Rieu I, Powers SJ. Real-Time Quantitative RT-PCR: Design, Calculations, and Statistics. *The Plant Cell*. 2009; 21:1031–3. doi: [10.1105/tpc.109.066001](https://doi.org/10.1105/tpc.109.066001) PMID: [19395682](https://pubmed.ncbi.nlm.nih.gov/19395682/)
39. Vandesompele J, Preter KD, Pattyn F, Poppe B, Roy NV, Paepe AD, et al. Accurate normalization of real-time quantitative RT-PCR data by geometric averaging of multiple internal control genes. *Genome Biology*. 2002; 3(7).